Electronic Supplementary Material (ESI) for Physical Chemistry Chemical Physics.

Identification of vanadium dopant sites in the Metal-Organic Framework DUT-5(Al): Supporting information.

Kwinten Maes[a], Lisa I. D. J. Martin[a], Samira Khelifi[a], Alexander Hoffman[b], Karen Leus[c], Pascal Van Der Voort[c], Etienne Goovaerts[d], Philippe F. Smet[a], Veronique Van Speybroeck[b], Freddy Callens[a] and Henk Vrielinck[a]

[a]Department of Solid State Sciences, Ghent University, Krijgslaan 281-S1, B-9000 Gent, Belgium. E-mail: henk.vrielinck@ugent.be

[b]Center for Molecular Modeling, Ghent University, Technologiepark 903, 9052 Zwijnaarde, Belgium.

[c]Department of Chemistry, Ghent University, Krijgslaan 281-S3, B-9000 Gent, Belgium

[d]Department of Physics, University of Antwerp, Universiteitsplein 1, B-2610 Antwerp, Belgium

Table of Contents

1. EPR spectra and simulations of additional samples

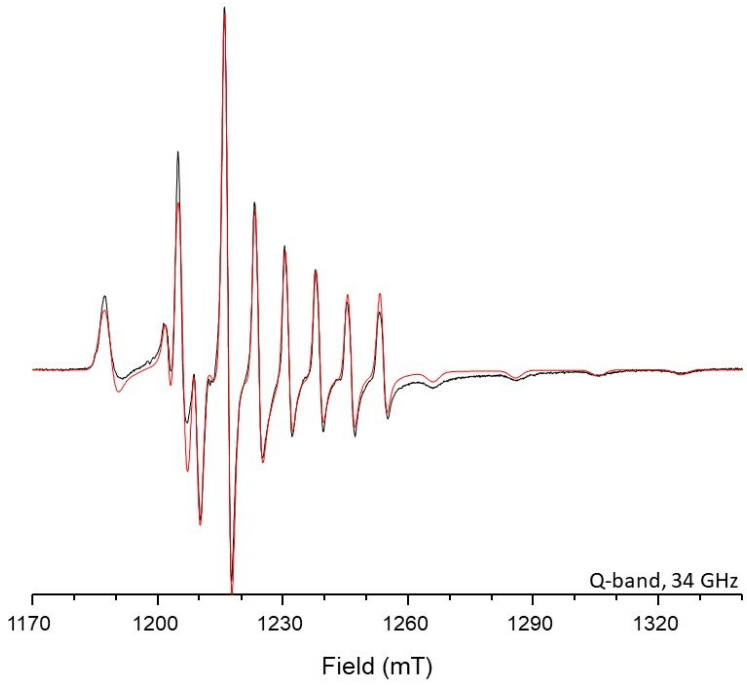

Figure S1: Q-band (34 GHz) 90 K EPR spectrum of the frozen solution of S-DMF-02: black – experiment; red – simulation. Spin-Hamiltonian parameters: g = [1.9774, 1.9770, 1.9334], A = [202.4, 196.2, 532.6] MHz. An anisotropic Gaussian linewidth was used for the simulations (HStrain = [46, 56, 92] MHz).

2. Decomposition of DUT-5(Al):V EPR spectra

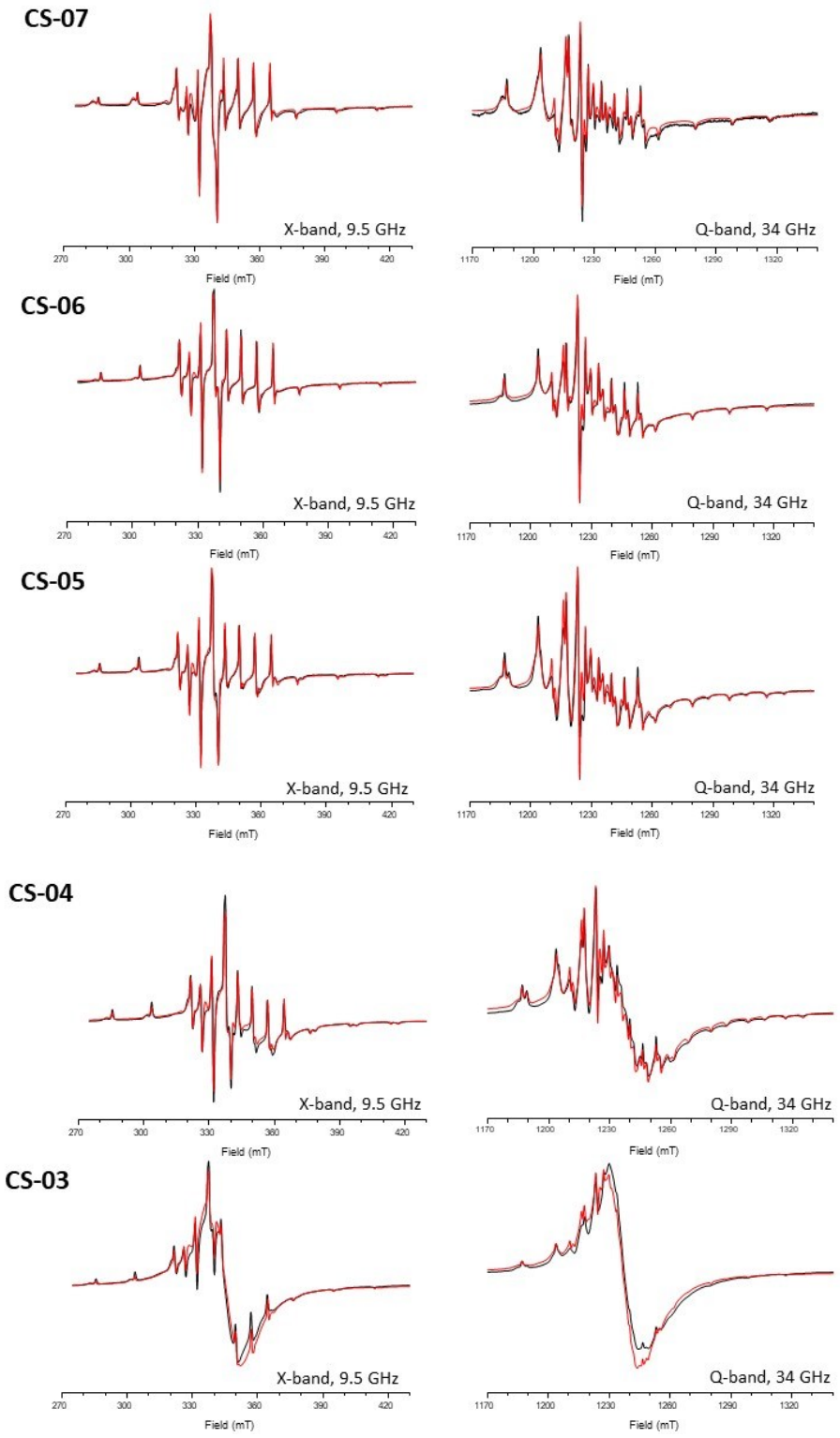

Figure S2: X- (left, 9.5 GHz) and Q-band (right, 34 GHz) RT powder EPR spectra of the CS samples measured in vacuum (≈ 30 Pa): black – experiment; red – simulation. The simulation is a linear combination of the simulated spectra of the four components ***lp***, ***BL/Blp***, ***np*** *and Lorentz, using the multiplication factors presented in Table S1.*

		X-band vacuum				Q-band vacuum			
Sample	%V	**lp**	**BL/Blp**	**np**	Lorentz	**lp**	**BL/Blp**	**np**	Lorentz
CS-07	3	162	215	3	-	496	589	36	-
CS-06	7	210	79	9	341	2448	895	219	6236
CS-05	9	189	149	32	255	2339	2191	929	5468
CS-04	23	286	250	101	1102	2349	2148	1456	17395
CS-03	46	189	146	34	1722	2383	2482	549	49581

Table S1: Simulated multiplication factors of each component as a function of the vanadium concentration (compared to the combined V and Al concentration, as measured by ICP-MS [1]) of the CS samples for the X-band (left) and Q-band (right) 30 Pa measurements. Each simulated component was multiplied with their multiplication factor to reconstruct the total measured EPR spectrum, as presented in Figure S3. Calculated relative error, based on repeated measurements, was 15% for all components.

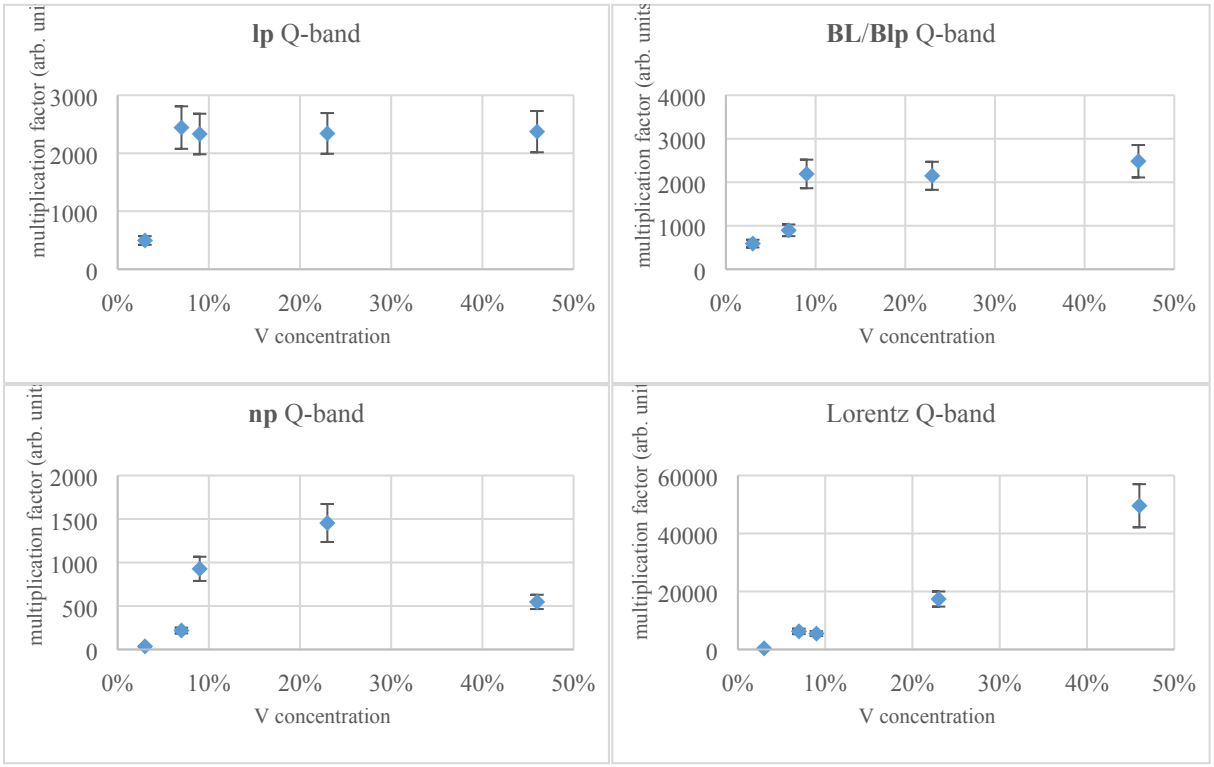

Figure S3: Simulated contribution of each component as a function of the vanadium concentration (compared to the combined V and Al concentration, as measured by ICP-MS [1]) of the CS samples for the Q-band 30 Pa measurements. Each simulated component was multiplied with these multiplication factors to reconstruct the total measured Q-band EPR spectrum. Calculated relative error, based on repeated measurements, was 15% for all components.

3. ENDOR

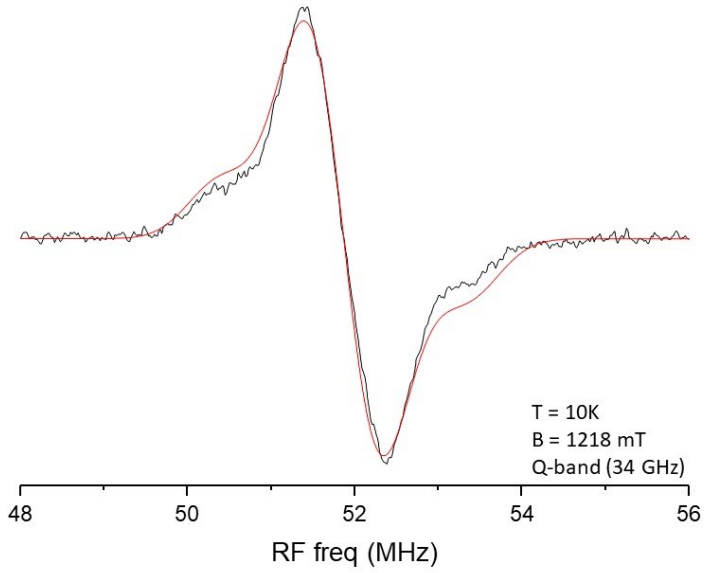

Figure S4: Q-band (34 GHz) 10K powder ^{1}H ENDOR spectrum of T-$VOSO_4$. black - experiment, red – simulation. A-tensor and linewidth parameter used for the simulation: A = [0, 0, 3.0] MHz, Lw = 0.9 MHz. Using the point-dipole approximation, this corresponds to a calculated V-H distance of 4.3 Å.

4. SEM-EDX

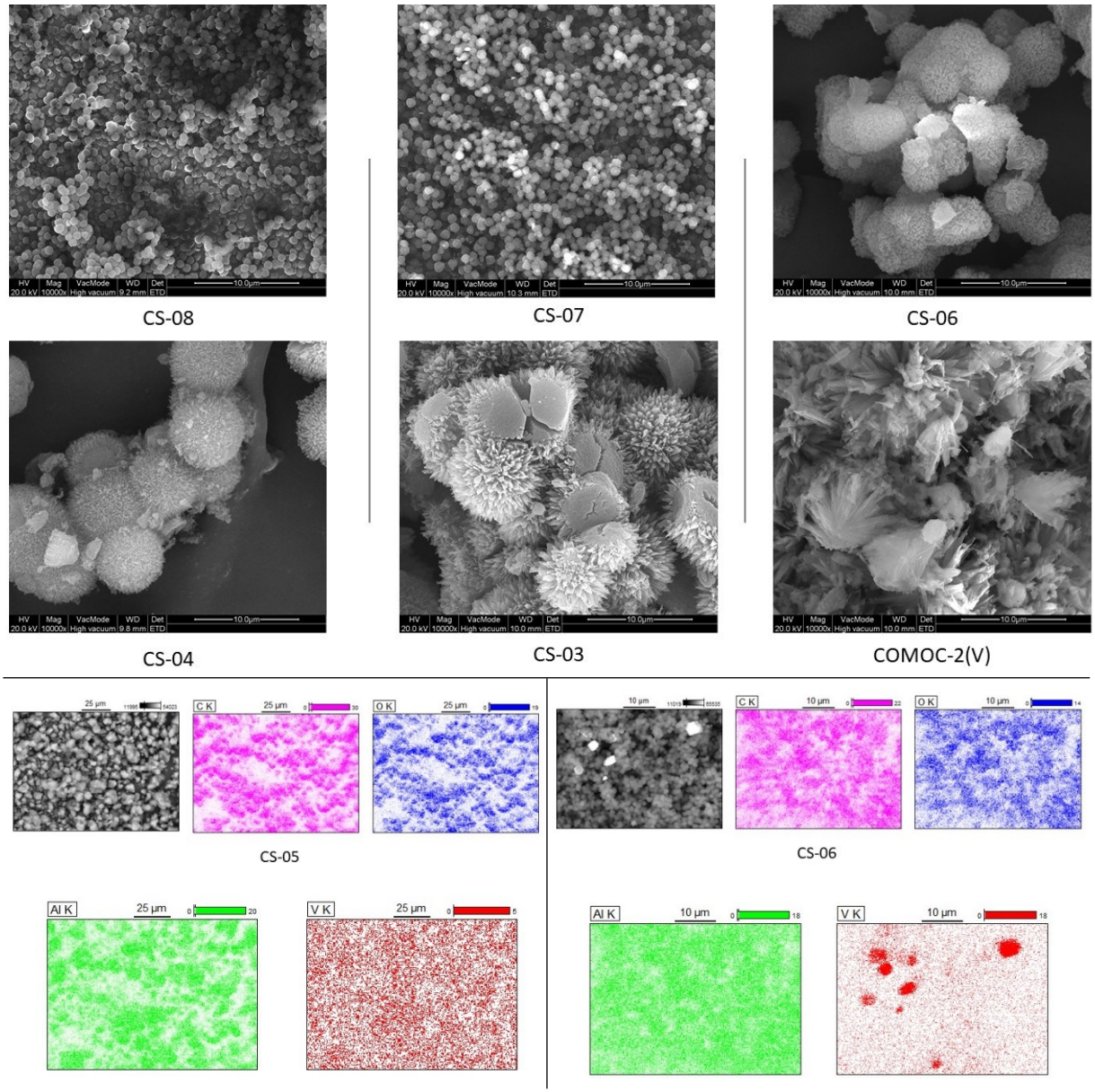

Figure S5: ***Top:*** *SEM images of CS samples and COMOC-2(V). The same magnification (scale indication = 10 µm) is applied for all images, showing an increase in grain size with increasing V concentration. CS-06 and CS-05 are similar in grain size.* ***Bottom left****: SEM-EDX mapping of CS-05. The images from left to right: SEM image (upper left), carbon mapping (upper middle), oxygen mapping (upper right), aluminum mapping (lower left), vanadium mapping (lower right). Mapping concentrations are calculated based on the intensities of the peaks of the measured EDX spectrum. The scale indication is 25 µm.* ***Bottom right****: SEM-EDX mapping of CS-06. The images from left to right: SEM image (upper left), carbon mapping (upper middle), oxygen mapping (upper right), aluminum mapping (lower left), vanadium mapping (lower right). Mapping concentrations are calculated based on the intensities of the peaks of the measured EDX spectrum. The scale indication is 10 µm.*

Sample	V concentration EDX (%)	V concentration ICP-MS (%)
CS-07	3.51 ± 0.26	3
CS-06	4.39* ± 0.48	7
CS-05	9.28 ± 0.39	9
CS-04	22.88 ± 12.12	23
CS-03	44.57 ± 6.44	46

*Table S2: Average vanadium concentration of the CS samples compared to the total vanadium and aluminum present as measured by ICP-MS [1] and EDX. The CS-06 EDX V concentration (indicated by *) is the average inside the MOF, excluding the clusters with higher V concentration (see Figure S5, bottom right, and main article). The error, calculated from repeated measurements at random points, gives an indication of the homogeneity of V concentration in the MOF.*

5. FTIR

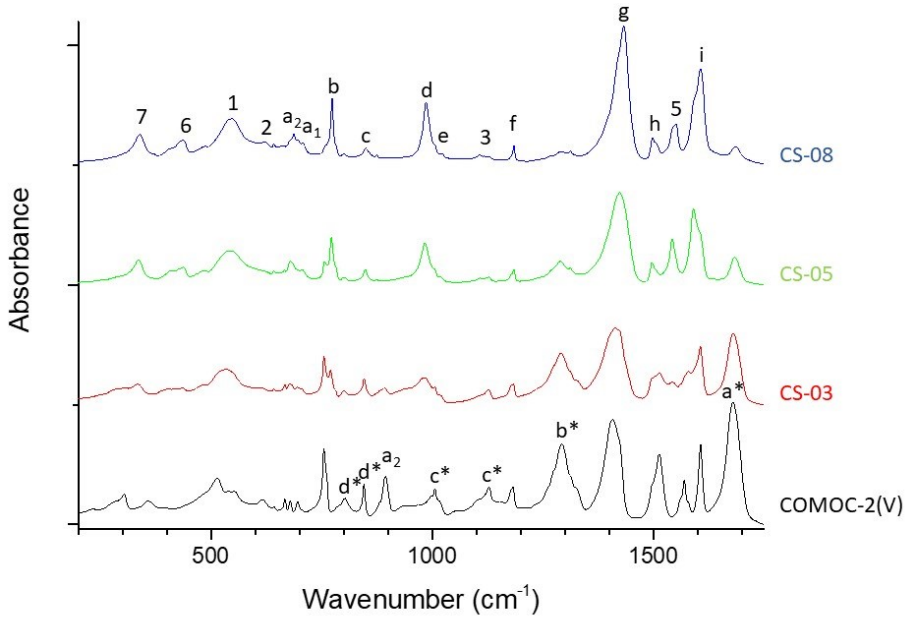

Figure S6: Attenuated total reflection FTIR spectra of COMOC-2(V) (black), CS-03 (red), CS-05 (green) and CS-08 (blue), in the 200-1750 cm^{-1} range. A full determination of the framework IR peaks was made based on first principles calculations (see Figure S9 and Table S3) and literature data (Hoffman et al. [2] on the isoreticular MIL-53(Al), Senkovska et al. [3] for DUT-5(Al), Depauw et al. [4] for COMOC-2(V) and Sienkiewicz-Gromiuk and Rzączyńska [5] for H_2BPDC).

Free linker molecule: In all IR spectra bands are visible of free linker molecules presumably present inside the framework pores. These IR bands are most prominent in the samples with higher V concentration. Around 1700 cm^{-1} (a*) a COOH stretch band is visible and CH bend bands are present around 1300 cm^{-1} (b*), 1150 cm^{-1} and 1000 cm^{-1} (c*). The IR bands between 900 and 800 cm^{-1} (d*) are originating from C-C-C bending of the benzene unit.

CS and COMOC-2(V) samples: In general OH and Al related IR bands are decreasing in relative intensity with increasing V concentration. The two bands around 1600 cm^{-1} (i) and 1550 cm^{-1} (5) originate from the antisymmetric CO_2 stretch combined with C-C stretch of the benzene unit. Around 1500 cm^{-1}, a combined C-C stretch and CH bend band is present (h). At higher V concentration, this band almost coincides with a new antisymmetric CO_2 stretch band. The band around 1400 cm^{-1} (g) originates from the symmetric CO_2 stretch and shifts to lower wavenumbers with higher V concentration. Another combined C-C stretch and CH bend band is present around 1200 cm^{-1} (f). There is a free OH bend band around 1000 cm^{-1} (d) that disappears with higher V concentration, revealing the underlying bands of the free linker molecules. The V=O antisymmetric stretch band is present around 900 cm^{-1} (a_2 COMOC-2(V)), as expected growing with increasing V concentration. Around 750 cm^{-1} (b) there is CH wagging band present that shifts towards lower wavenumbers with increasing V concentration. The symmetric and antisymmetric O-Al-O stretch bands present around 700 cm^{-1} (a_1 and a_2 DUT-5(Al)) disappear with increasing V concentration, revealing three small underlying bands: the band at highest wavenumber originates from CH wagging and the lower frequency modes are due to bending of the CO_2 unit and to C-C-C bending in the benzene units.

The far-IR region of DUT-5(Al) and COMOC-2(V) is characterized by the same three types of vibrational modes, which were also observed in MIL-53(Al). Around 500 cm^{-1} (1) there are the metal-oxide stretch bands. Some of the bands are coupled with out-of-plane vibrations of the benzene units. Around 400 cm^{-1} (6) there are bands of the metal-oxide bending modes and around 300 cm^{-1} (7) the vibration modes are dominated by translations of the metals along the metal-oxide chain, which also induces translation of the linker.

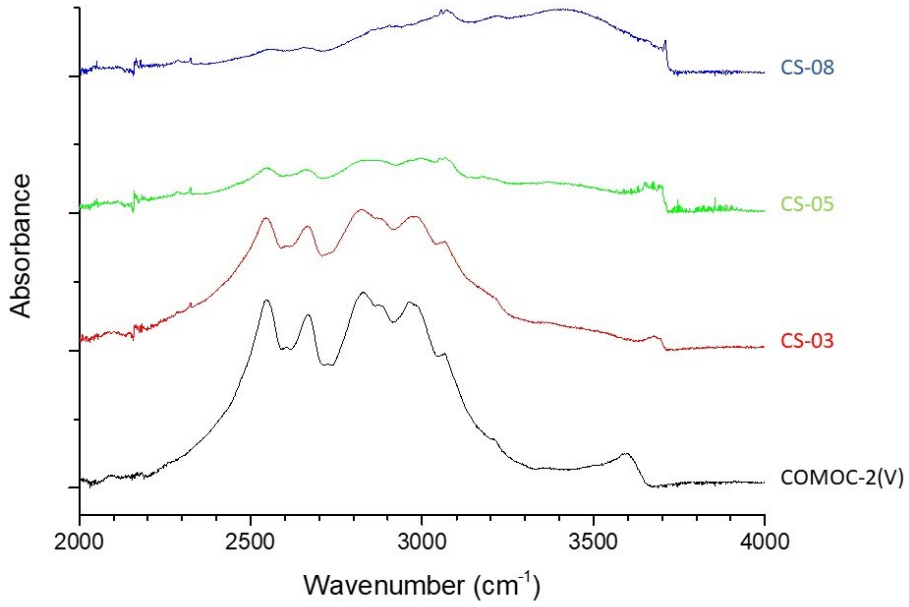

Figure S7: Attenuated total reflection FTIR spectra of COMOC-2(V) (black), CS-03 (red), CS-05 (green) and CS-08 (blue), in the 2000-4000 cm^{-1} range.

Between 2400 and 3200 cm^{-1} multiple IR bands are visible originating from free linker molecules trapped inside the framework pores. These bands are most pronounced in the samples with higher V concentration. Around 3700 cm^{-1} in DUT-5(Al) there is a sharp IR band visible that is originating in from the OH stretch vibration of the hydroxyl groups in the Al-OH-Al chains. With increasing V concentration this sharp IR band disappears and a broader band appears around 3600 cm^{-1} possibly related to free water inside the framework pores.

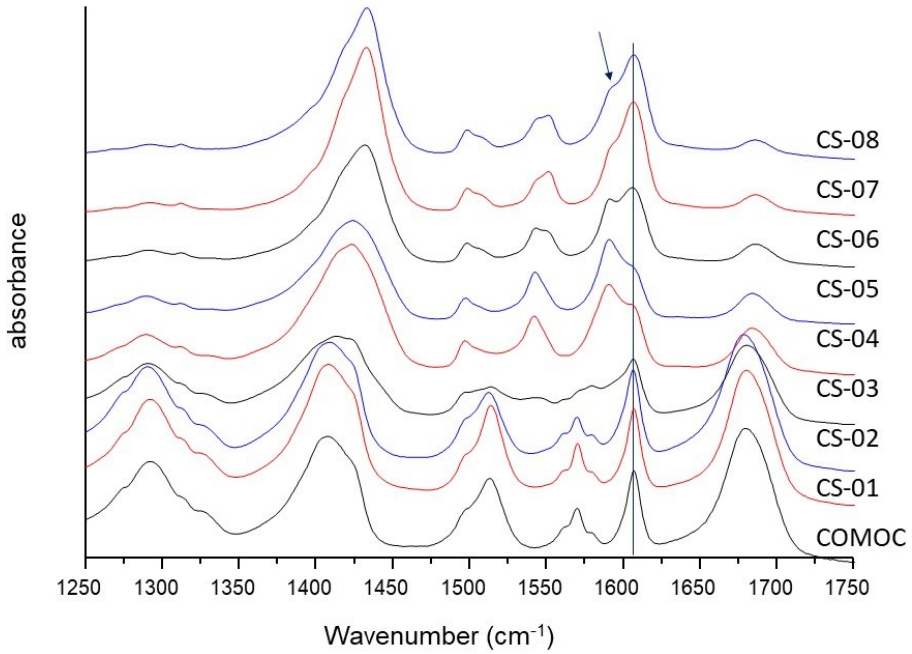

*Figure S8: Attenuated total reflection FTIR spectra of the CS samples and COMOC-2(V), in the 1250-1750 cm^{-1} range. The line shows the antisymmetric CO_2 stretch peak for the **lp** phase. The arrow points towards the antisymmetric CO_2 stretch peak for the **np** phase, which is red-shifted compared to the **lp** phase peak.*

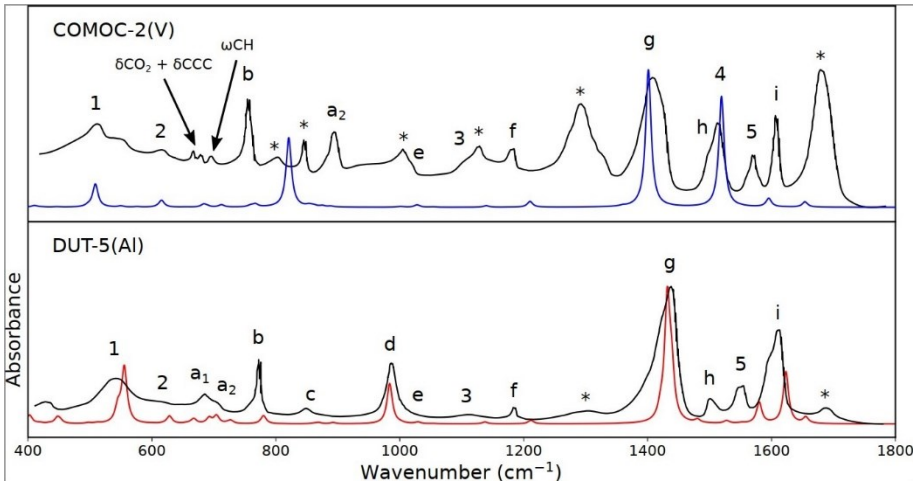

*Figure S9: Mid-IR spectra of COMOC-2(V) (top) and DUT-5(Al) (bottom) in the range 400-1800 cm^{-1}. Experimental IR spectra are represented in black. Static DFT results of the **lp** phases are colored and scaled in frequency with a scaling factor of 1.03 [2]. The labels with letters are the same as those presented in Hoffman et al. [2] for MIL-53(Al), while the labels with numbers characterize additional IR bands. Their assignation can be found in Table S3. IR active modes due to residual BPDC linker are labeled with *.*

Vibrational mode	Assignation	DUT-5(Al)			COMOC-2(V)		
		np	lp	exp	np	lp	exp
1	$\nu_{O_C}MO_C$	552	555	550	506	509	520
2	$\nu_{O_C}MO_C$	616	628	625	604	616	620
a1	ν_{sym}MOM	661	667	645			
a2	ν_{as}MOM	693	705	680	803	821	895
b	ωCH	779	781	775	764	766	755
c	δCCC + δCO_2	862	865	850	874	876	850
d	δOH	992	984	985			
e	δCCC + δCH	1030	1029	1005	1029	1028	1005
3	δCH	1144	1137	1130	1142	1139	1130
f	$\nu CC_+ \delta$CH	1215	1211	1180	1213	1210	1180
g	$\nu_{sym}CO_2$	1424	1432	1425	1395	1402	1405
h	$\nu CC_+ \delta$CH	1526	1527	1500	1521	1524	1500
4	$\nu_{as}CO_2$				1507	1519	1510
5	$\nu_{as}CO_2 + \nu$CC	1570	1580	1550	1594	1595	1570
i	$\nu_{as}CO_2 + \nu$CC	1611	1623	1605	1620	1624	1605

Table S3: Assignation of IR active modes of DUT-5(Al) and COMOC-2(V) in the mid-IR region, based on the simulations presented in Figure S9 and the experimental spectra in Figure S6. Simulated data are scaled with a scaling factor of 1.03 [2]. Frequencies are given in cm^{-1}.

6. Annealing experiments

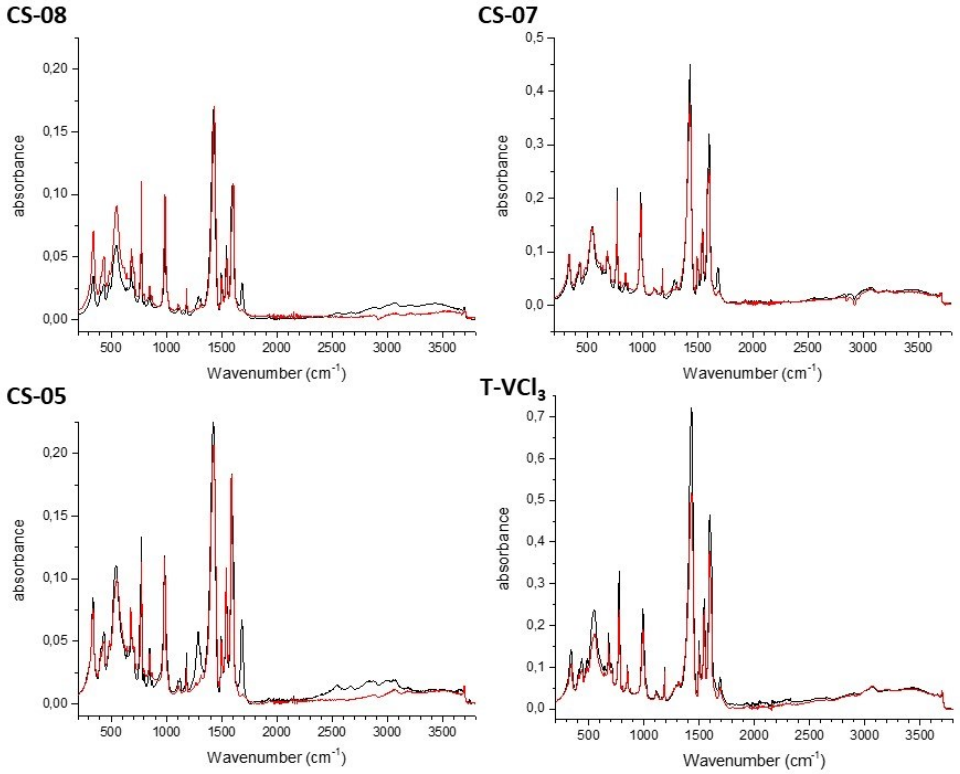

Figure S10: Attenuated total reflection FTIR spectra of CS-08 (left up), CS-07 (right up), CS-05 (left down) and T-VCl_3 (right down): black – before calcination; red – after calcination.

X-band vacuum					
Sample	**lp**	**BL/Blp**	**np**	Lorentz	Giso
CS-08	78	85	1	-	-
CS-08-H	96	70	9	-	6
CS-07	162	215	3	-	-
CS-07-H*	255	748	44	-	14
CS-05	189	149	32	255	-
CS-05-H	136	128	42	237	6
T-VCl_3	24	250	16	-	-
T-VCl_3-H*	58	419	53	-	7

Table S4: Simulated multiplication factors of each component as a function of the vanadium concentration (compared to the combined V and Al concentration, as measured by ICP-MS [1]) of CS-08, CS-07, CS-05 and T-VCl_3 before and after calcination for the X-band 30 Pa measurements. Component Giso refers to the isotropic line with g = 2.004 present in the EPR spectra after calcination. Each simulated component was multiplied with the tabulated multiplication factor to reconstruct the total measured EPR spectrum, as presented in Figure S11. For the two calcined samples CS-07-H and T-VCl_3-H the sample quantity differed strongly from the non-calcined CS-07 and T-VCl_3 samples, therefore only the comparison of the ratios of the multiplication factors is relevant. Calculated relative error, based on repeated measurements, was 15% for all components.

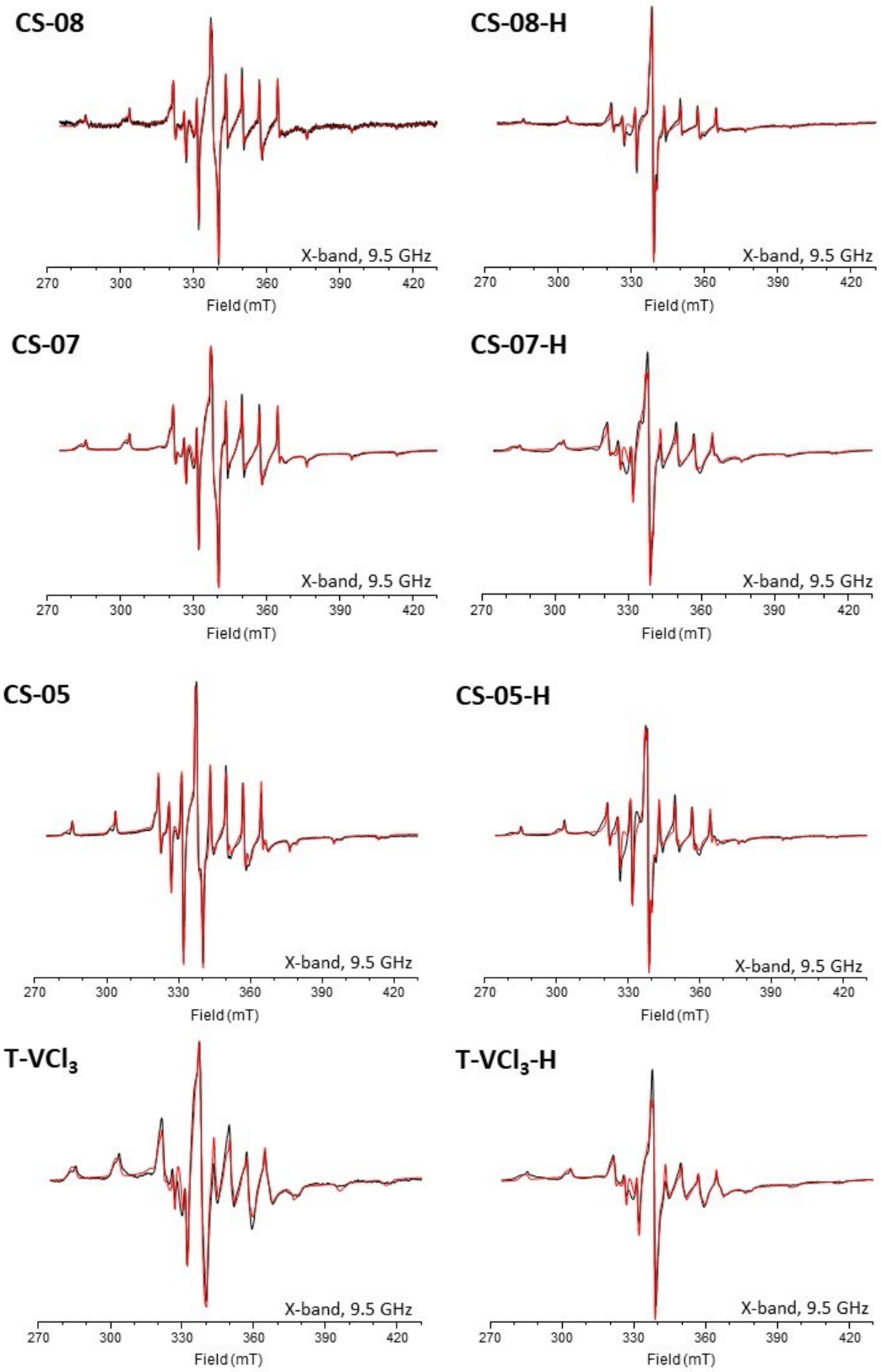

Figure S11: X- band (9.5 GHz) RT powder EPR spectra of the CS-08, CS-07, CS-05 and T-VCl3 samples before (left) and after (right) calcination measured in vacuum (≈ 30 Pa): black – experiment; red – simulation. The simulation is a linear combination of the simulated spectra of the four components ***lp***, ***BL/Blp***, ***np*** *and Lorentz, using the multiplication factors presented in Table S4.*

7. XRD

	DUT-5(Al)		COMOC-2(V)		CS-08 - CS-04
	EXP	MM	EXP	MM	EXP
LP (110)	6.02°	6.31°	6.04°	5.94°	6.05°
NP (002)	6.38°	6.35°	6.37°	6.28°	6.35°
LP (220)	12.05°	12.64°	12.10°	11.88°	12.05°
NP (004)	12.78°	12.72°	12.78°	12.59°	12.80°

Table S5: XRD diffraction angle calculated from crystallographic data, both the experimental (EXP) and molecular modeling (MM) data, for DUT-5(Al) [6] and COMOC-2(V) [7]. XRD diffraction angles for the CS samples were estimated from Figure S12. Error margin 0.05°.

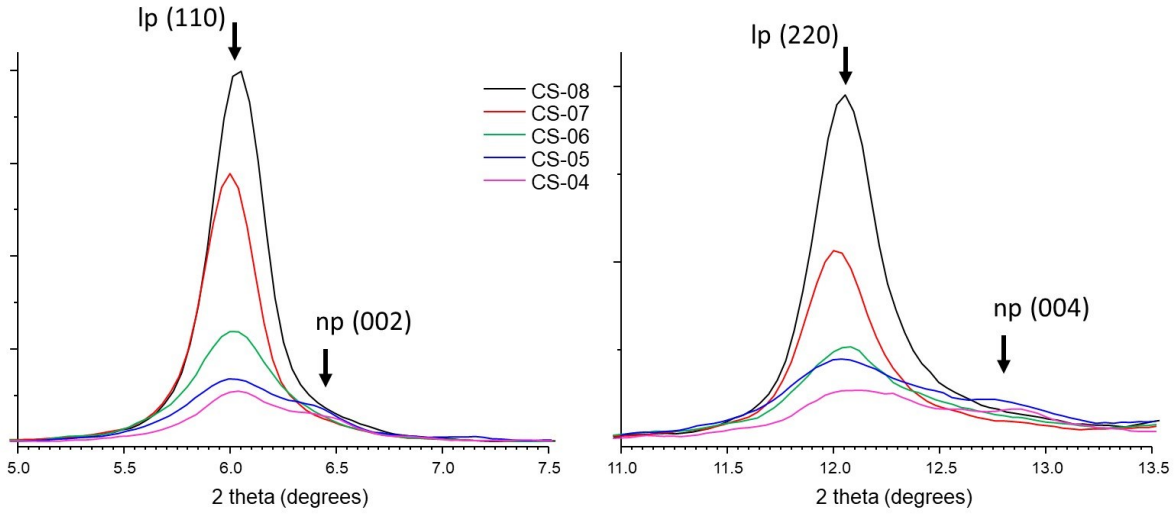

*Figure S12: V concentration dependence of XRD patterns of DUT-5(Al) in air in two different 2ϑ regions, λ = 1.54056 Å. Miller indices for the peaks related to **lp** and **np** are indicated. Reproduced from Maes et al. [8].*

1. Depauw, H., et al., *Discovery of a novel, large pore phase in a bimetallic Al/V metal–organic framework.* Journal of Materials Chemistry A, 2017. **5**(47): p. 24580-24584.
2. Hoffman, A.E.J., et al., *Elucidating the Vibrational Fingerprint of the Flexible Metal-Organic Framework MIL-53(Al) Using a Combined Experimental/Computational Approach.* J. Phys. Chem. C, 2018. **122**(5): p. 2734-2746.
3. Senkovska, I., et al., *New highly porous aluminium based metal-organic frameworks: Al(OH)(ndc) (ndc = 2,6-naphthalene dicarboxylate) and Al(OH)(bpdc) (bpdc = 4,4'-biphenyl dicarboxylate).* Microporous and Mesoporous Materials, 2009. **122**(1–3): p. 93-98.
4. Depauw, H., *Investigation of the Doping Effect in Bimetallic Metal-organic Frameworks to Tune Their Structural Flexibility*, in *Faculty of Sciences*. 2018, Ghent University: Ghent, Belgium.
5. Sienkiewicz-Gromiuk, J. and Z. Rzączyńska, *Structural, thermal, and spectral investigations of the lanthanide(III) biphenyl-4,4'-dicarboxylates.* Journal of Thermal Analysis and Calorimetry, 2012. **112**(2): p. 877-884.
6. Wieme, J., *Advanced Molecular Simulations to Computationally Model Phase Stability and Thermal Properties of Metal-Organic Frameworks*, in *Faculty of Engineering and Architecture*. 2020, Ghent University. p. 330.
7. Liu, Y.Y., et al., *New V(IV)-based metal-organic framework having framework flexibility and high CO2 adsorption capacity.* Inorg. Chem., 2013. **52**(1): p. 113-20.
8. Maes, K., et al., *EPR characterization of vanadium dopant sites in DUT-5(Al).* Optical Materials, 2019. **94**: p. 217-223.